THE JOURNAL OF BIOLOGICAL CHEMISTRY Vol. 278, No. 41, Issue of October 10, pp. 40050–40056, 2003

Printed in U.S.A.

The MinD Membrane Targeting Sequence Is a Transplantable Lipid-binding Helix*

Received for publication, June 27, 2003, and in revised form, July 25, 2003
Published, JBC Papers in Press, July 25, 2003, DOI 10.1074/jbc.M306876200

Tim H. Szeto‡, Susan L. Rowland‡, Cheryl L. Habrukowich‡, and Glenn F. King‡§¶

From the Departments of ‡Biochemistry and §Microbiology, University of Connecticut Health Center, Farmington, Connecticut 06032

MinD is a ubiquitous ATPase that plays a crucial role in selection of the division site in eubacteria, chloroplasts, and probably also Archaea. It was recently demonstrated that membrane localization of MinD is mediated by an 8–12-residue C-terminal motif termed the membrane targeting sequence or MTS. In this study we show that the MinD MTS is a transplantable lipid-binding motif that can effectively target heterologous proteins to the cell membrane. We demonstrate that eubacterial MTSs interact directly with lipid bilayers as an amphipathic helix, with a distinct preference for anionic phospholipids. Moreover, we provide evidence that the phospholipid preference of each MTS, as well as its affinity for biological membranes, has been evolutionarily "tuned" to its specific role in different bacteria. We propose a model to describe how the MTS is coupled to ATP binding to regulate the reversible membrane association of *Escherichia coli* MinD during its pole-to-pole oscillation cycle.

The initiating event in bacterial cytokinesis is the formation of a circumferential ring of polymerized FtsZ, the ancestral homolog of eukaryotic tubulin (1–3). The FtsZ ring provides a scaffold onto which numerous proteins are subsequently assembled to form the functional division apparatus (4, 5). In the rod-shaped bacterium *Escherichia coli*, placement of the FtsZ ring, and thus the division septum, is negatively regulated by the three proteins encoded by the *minB* operon: MinC, MinD, and MinE (3, 6, 7). In the absence of the Min system, FtsZ rings can form either at midcell or in the nucleoid-free regions at either of the cell poles (8). Polar divisions are nonproductive as they lead to the formation of chromosomeless minicells and multinucleate filaments.

MinC and MinD associate to form an indiscriminate division inhibitor whose activity is restricted to polar sites in *E. coli* by the action of MinE (6). Studies of GFP[1]-labeled Min proteins from the Gram-negative bacteria *E. coli* and *Neisseria gonorrhoeae* have revealed that they undergo a remarkable pole-to-pole oscillation that causes the time-averaged concentration of the MinCD division inhibitor to be lowest at midcell (9–15). This makes midcell the preferred site for construction of an FtsZ ring. In contrast, *Bacillus subtilis* and most other Gram-positive bacteria lack the MinE protein that promotes MinCD oscillation in *E. coli*. Instead, in *B. subtilis*, the MinCD complex is anchored at the cell poles by DivIVA where it remains throughout the cell cycle until a late stage in assembly of the division apparatus when it is piloted to the nascent division site (16–18).

MinD is a peripheral membrane protein (19), and its association with the inner membrane is a prerequisite for subsequent membrane recruitment of MinC (and MinE in *E. coli*). MinD is a member of the ParA superfamily of ATPases that are characterized by a deviant Walker A motif (19–22). The ATPase activity of MinD provides the driving force for oscillation of the Min proteins in *E. coli*; this activity is stimulated by MinE but only in the presence of phospholipids (23–25). *In vitro*, in the presence of ATP and phospholipid vesicles, MinD forms unbranched protofilaments and filament bundles (25) as well as tubes that appear to comprise a helical array of MinD molecules (24). However, in live *E. coli* cells, MinD appears to be organized into extended coiled structures that wind around the inner membrane, with each coil presumed to consist of bundled protofilaments (26).

The mechanism by which MinD associates with the inner membrane proved enigmatic for more than a decade. However, it was recently demonstrated that MinD is targeted to the membrane by a short C-terminal motif (27, 28) that we refer to as the membrane targeting sequence or MTS. We postulated that this motif, which is conserved across phyla, forms a short amphipathic α-helix that mediates a direct interaction between MinD and membrane phospholipids (27). However, this raises a number of fundamental questions. How does the MTS recognize biological membranes with different phospholipid composition? How can the MTS facilitate permanent membrane association of *B. subtilis* MinD (*Bs*MinD) but allow for rapid cycles of membrane attachment-detachment in the case of *E. coli* MinD (*Ec*MinD)? Can the MTS function as an autonomous membrane-targeting motif?

In this study, we show that the MinD MTS interacts directly with lipid bilayers as an amphipathic helix, and that it can function as a transplantable membrane-targeting motif. Moreover, we provide evidence that the phospholipid preference and membrane affinity of each MTS has been "tuned" to its specific role in different bacteria. We propose a new model to describe how the MTS is coupled to ATP binding to regulate the reversible membrane association of *Ec*MinD during its oscillation cycle.

* This work was supported by NIAID National Institutes of Health Grant AI-048583 (to G. F. K.). The costs of publication of this article were defrayed in part by the payment of page charges. This article must therefore be hereby marked "*advertisement*" in accordance with 18 U.S.C. Section 1734 solely to indicate this fact.

¶ To whom correspondence should be addressed: Dept. of Biochemistry, University of Connecticut Health Center, 263 Farmington Ave., Farmington CT 06032-3305. Tel.: 860-679-8364; Fax: 860-679-1652; E-mail: glenn@psel.uchc.edu.

[1] The abbreviations used are: GFP, green fluorescent protein; *Bs*MinD, *Bacillus subtilis* MinD; *Bs*MTS, *B. subtilis* membrane targeting sequence; CL, cardiolipin; *Ec*MinD, *Escherichia coli* MinD; *Ec*MTS, *E. coli* membrane targeting sequence; MTS, membrane targeting sequence; PC, phosphatidylcholine; PE, phosphatidylethanolamine; PG, phosphatidylglycerol; SUV, small unilamellar vesicle; WT, wild-type; LZ, leucine zipper.

EXPERIMENTAL PROCEDURES

Peptide Synthesis—Peptides corresponding to residues 256–270 of *Ec*MinD (*Ec*MTS$^{256-270}$), *Ec*MTS$^{256-270}$ with an L267E mutation (*Ec*MTS^{L267E}), residues 248–268 of *Bs*MinD (*Bs*MTS$^{248-268}$), and *Bs*MTS$^{248-268}$ with a randomized amino acid sequence (IKVSVFNESRAEFGLKQGMKM; *Bs*MTS^{scramble}) were synthesized using Fmoc (*N*-(9-fluorenyl)methoxycarbonyl) solid phase peptide synthesis by Auspep (Victoria, Australia). The C terminus of these peptides corresponds to the C terminus of the native MinD proteins. The N terminus of the peptides was acetylated to avoid introduction of a non-native charge that would be unfavorable to helix formation (29). Correct products were verified by electrospray mass spectrometry then purified using reverse-phase high performance liquid chromatography. The stock concentration of each peptide for circular dichroism (CD) experiments was determined by amino acid analysis.

Preparation of Small Unilamellar Vesicles (SUVs)—Chicken egg phosphatidylcholine (PC) and phosphatidylglycerol (PG), bovine heart cardiolipin (CL), and *E. coli* phosphatidylethanolamine (PE) were purchased from Avanti Polar Lipids (Alabaster, AL). SUVs were prepared as described previously (30) with minor modifications. Briefly, lipids in $CHCl_3$ were mixed at the desired ratio in glass vials and dried under argon before further drying under vacuum. The dried lipids were rehydrated for 1 h at ambient temperature in CD buffer (1 mM NaH_2PO_4, 50 mM NaF, pH 7.4) to a final concentration of 10 mg ml^{-1}, before sonicating for 20–30 min in a bath sonicator (Fisher) until the solution became clear. SUVs were used for CD experiments on the day they were prepared.

CD Spectropolarimetry—Far-UV CD spectra were acquired at 25 °C on a Jasco J-715 spectropolarimeter (Jasco, Easton, MD). Peptide and lipid samples were mixed thoroughly in CD buffer in a 0.5-mm pathlength quartz cuvette (Hellma, New York). The peptide:SUV molar ratio was at least 1:50. Spectra were the average of 9 scans acquired using a scan rate of 20 nm min^{-1} and a response time of 8 s. Background signal (buffer only or lipid only) was subtracted from the spectra before expressing values as mean residue molar ellipticity (θ, degrees cm^2 dmol^{-1}). The percent α-helix of each peptide was estimated from the CD spectra according to the following equation (31, 32),

$$f_h = \theta_{222}/\theta_{222\infty} + ik/N \quad \text{(Eq. 1)}$$

where f_h is the percent helicity of the peptide, θ_{222} is the mean residue ellipticity of the peptide at 222 nm, $\theta_{222\infty}$ is the mean residue ellipticity at 222 nm of an α-helix of infinite length ($-39{,}500$ degrees cm^2 dmol^{-1}), i is the number of α-helices (assumed to be 1), k is a wavelength-specific constant with a value of 2.6 at 222 nm, and N is the number of residues in the peptide. Although Equation 1 was derived from CD spectra of standard proteins dissolved in aqueous solution, it has been used extensively to estimate the helix content of peptides bound to lipid bilayers (30, 33–35).

Construction of GFP Fusions—All GFP constructs used in this study were placed downstream of the P_{ara} promoter and were therefore inducible with arabinose. We used the *gfpmut2* gene for all GFP constructs (36). A GFP fusion to *Ec*MTS$^{252-270}$ (GFP-*Ec*MTS) was generated by PCR using pSLR22 (12), a pBAD33-derived plasmid encoding P_{ara}-GFP::*Ec*MinD, as the template and primers that incorporated flanking *Xba*I/*Hin*dIII restriction sites. This allowed the excision of *Ec*MinD from pSLR22 and replacement by *Ec*MTS$^{252-270}$ to yield plasmid pTS14 encoding P_{ara}-GFP::*Ec*MTS$^{252-270}$.

Fusions between GFP and tandem repeats of the *Ec*MTS were constructed as follows. *Ec*MTS DNA was used as a template in a PCR with 5′ and 3′ primers to create a fragment that encoded the following sequence: *Xba*I-GGA-*Bgl*II-*Ec*MTS-GGT-*Bam*HI-TAG-*Hin*dIII. This fragment was digested with *Xba*I/*Hin*dIII and inserted into *Xba*I/*Hin*dIII-cut pSLR22, yielding a plasmid (pSLR91) that expressed GFP fused at the C terminus to the augmented *Ec*MTS fragment SRGRS-FIEEEKKGFLKRLFGGGGS (the native *Ec*MTS sequence, corresponding to residues 255–270, is underlined). pSLR92 was created by cutting the same PCR fragment with *Xba*I/*Bam*HI, and ligating it to *Xba*I/*Bgl*II-digested pSLR91. This plasmid expresses a tandem repeat of the *Ec*MTS fused to the C terminus of GFP (*i.e.* a C-terminal FIEEEKKGFLKRLFGGGGS sequence is added to the fusion protein encoded by pSLR91). An iteration of the process using pSLR92 as the backbone produced pSLR93. Thus pSLR91, -92, and -93 express GFP fused to 1, 2, and 3 repeats of *Ec*MTS$^{255-270}$, respectively, with each repeat separated by a Gly-Gly-Ser linker.

*Bs*MTS$^{248-268}$ was obtained by PCR using pTS26 (which encodes the full-length *B. subtilis minD* gene) as template (27) and 5′ and 3′ primers incorporating *Xba*I and *Pst*I restriction sites, respectively. This construct was then ligated into an *Xba*I/*Pst*I-digested pTS26 to yield plasmid pCLH1 in which *Bs*MTS$^{248-268}$ is encoded as an in-frame fusion to the C terminus of GFP (GFP::*Bs*MTS). GFP-*Ec*MinC-*Bs*MTS was constructed as follows: PCR was used to generate *Bs*MTS$^{248-268}$ with flanking 5′-*Sac*I and 3′-*Hin*dIII sites, and *Ec*MinC incorporating 5′-*Xba*I and 3′-*Sac*I sites. The two products were ligated into *Xba*I/*Hin*dIII-digested pTS14 to yield pCLH2 encoding *Ec*MinC-*Bs*MTS$^{248-268}$ appended to the C terminus of GFP. A triglycine linker was included between *Ec*MinC and *Bs*MTS$^{248-268}$ to allow for torsional flexibility. A similar strategy was used to construct GFP-JunLZ-*Ec*MTS$^{256-270}$ (pTS37) and GFP-JunLZ (pTS38). Briefly, the leucine zipper domain of the human transcription factor c-Jun (JunLZ) was generated by PCR using a plasmid encoding a homodimerization-enhanced JunLZ mutant (A298I) as template (37). The resulting PCR product incorporated flanking 5′-*Xba*I and 3′-*Pst*I sites. This PCR product, along with a PCR-generated *Ec*MTS$^{256-270}$ construct incorporating 5′-*Pst*I and 3′-*Hin*dIII sites, was then ligated into pTS14 as described above.

Fluorescence Microscopy—Visualization of GFP fusion constructs was performed exactly as described previously (27) using the *E. coli* host strain PB114 (6) that contains a deletion of the *minB* operon.

RESULTS

The MinD MTS Becomes Helical Upon Interaction with Lipid Bilayers—We recently proposed that the MinD MTS interacts directly with lipids as an amphipathic helix such that residues on the hydrophobic face insert into the bilayer, whereas cationic residues on the polar face of the helix interact preferentially with the head groups of anionic phospholipids (27). To test this hypothesis, we used CD spectropolarimetry to examine the ability of peptides encompassing the MTS of *E. coli* and *B. subtilis* MinD to interact directly with lipid bilayers present in the form of SUVs.

In the absence of lipids, both the *Ec*MTS$^{256-270}$ and *Bs*MTS$^{248-268}$ peptides exhibited CD spectra with a single minimum at 200 nm that is characteristic of a random coil (Fig. 1, *A* and *C*, respectively). That is, in the absence of lipid bilayers, neither the *E. coli* nor the *B. subtilis* MTS peptides exhibit any stable secondary structure. This is consistent with the observation that the C-terminal 30 residues of *Archaeoglobus fulgidus* MinD are highly disordered when the protein is crystallized in the absence of lipids (38).

We initially examined the interaction of MTS peptides with SUVs containing a mixture of lipids (70% PE, 20% PG, 10% CL) that approximated the known phospholipid ratio in the *E. coli* inner membrane (39, 40); we refer to these as "wild-type" SUVs (WT-SUVs). Addition of WT-SUVs to the *Ec*MTS$^{256-270}$ peptide caused a significant alteration in the CD spectrum; the minimum at 202 nm was slightly blue-shifted to 204 nm, and the minimum at 222 nm became more pronounced (Fig. 1*A*). This indicates that the *Ec*MTS$^{256-270}$ peptide interacts directly with lipid bilayers, and the enhanced intensity of the peak at 222 nm indicates that this interaction causes the MTS to become at least partially helical. Similar random coil → helix transitions in the presence of phospholipid bilayers (41) have been reported for the membrane-targeting sequences of the mammalian GTPase RGS4 (30) and the *E. coli* enzyme IIA^{Glucose} (42). The ellipticity at 222 nm indicates that the *Ec*MTS$^{256-270}$ peptide is, on average, 35–40% helical, which corresponds to about 1.5 helical turns (5–6 residues).

We previously showed that mutating Leu^{267} to Glu, which interrupts the hydrophobic surface of the putative MTS helix by introducing a charged residue (see helical wheel in Fig. 1*B*), resulted in *Ec*MinD no longer being targeted to the membrane (27). A peptide incorporating this mutation (*Ec*MTS^{L267E}) is unstructured both in the absence of lipids and in the presence of WT-SUVs (Fig. 1*B*). We conclude that the amphipathic nature of the MTS helix is critical for its interaction with lipids.

Addition of WT-SUVs to the *Bs*MTS$^{248-268}$ peptide caused a more dramatic alteration in the CD spectrum than observed with the *Ec*MTS$^{256-270}$ peptide; the minimum at 200.5 nm was

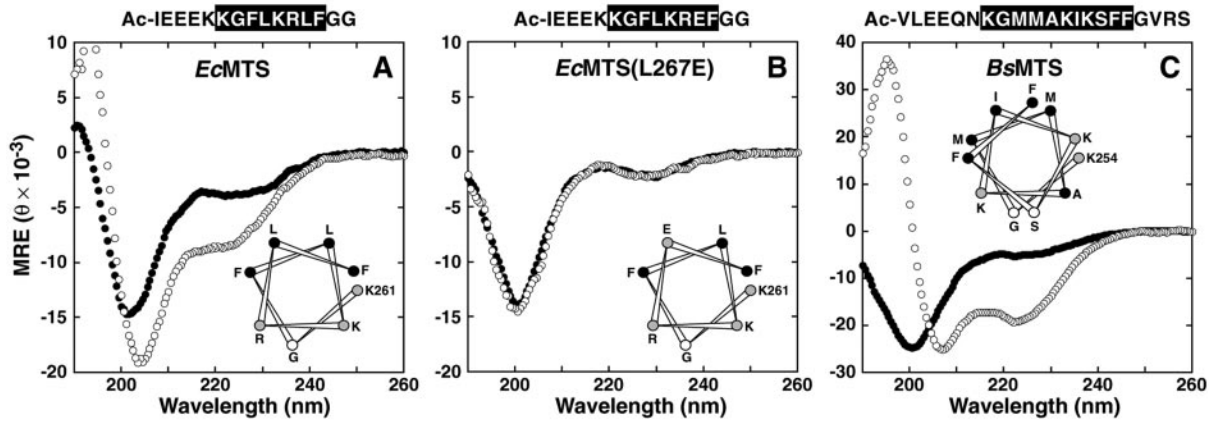

FIG. 1. **Far-UV circular dichroic spectra of *Ec*MTS$^{256-270}$ (*A*), *Ec*MTS^{L267E} (*B*), and *Bs*MTS$^{248-268}$ (*C*) peptides in the absence (●) and presence (○) of WT-SUVs.** The SUV:peptide molar ratio was ~50:1. Peptide sequences are given *above* the spectra with the minimal MTS (27) highlighted in *reverse type*. Note that the N termini of the peptides were acetylated (*Ac*). The MTS regions are displayed on the spectra as helical wheels, with hydrophobic and charged residues indicated by *black* and *gray circles*, respectively. *MRE* is the mean residue ellipticity in units of degrees cm^2 dmol^{-1}.

significantly blue-shifted to 207.5 nm, and the minimum at 222 nm became much more pronounced (Fig. 1*C*). The helicity calculated from the ellipticity at 222 nm is ~60%; this corresponds to about 3.5 helical turns (12–13 residues), which is the predicted size of the *B. subtilis* MTS (27). A peptide containing a scrambled version of the *Bs*MTS sequence (*Bs*MTS^{scramble}) was unstructured both in the absence of lipids and in the presence of WT-SUVs (data not shown). This indicates that the specific sequence of residues in the MTS, and not just the properties of the amino acid side chains, is critical for membrane binding.

We conclude that both the *E. coli* and *B. subtilis* MTS interact directly with phospholipid bilayers as amphipathic α-helices. The percent helix calculated using Equation 1 should be considered only an approximation of the absolute helicity of each MTS peptide. However, the substantial difference in the estimated helicities of the *Ec*MTS$^{256-270}$ and *Bs*MTS$^{248-268}$ peptides in the presence of WT-SUVs is nonetheless real as evidenced by the marked difference in intensity of the characteristic α-helical signature at 222 nm in the CD spectra of the peptides mixed with SUVs.

There are several possible interpretations of this apparent difference in helicity. First, it might indicate a significant difference in the length of the helices formed by the *Ec*MTS and *Bs*MTS peptides when they bind lipid bilayers. We think this interpretation is unlikely, as the apparent helix content of the *Ec*MTS$^{256-270}$ peptide when bound to SUVs is only ~1.5 helical turns according to Equation 1, and we are unaware of any previously documented interaction between such a small helix and lipid membranes. The alternative explanation that we favor is that the helices formed by the *Bs*MTS and *Ec*MTS peptides are of similar size and that the more dramatic CD spectral changes observed for the *Bs*MTS$^{248-268}$ peptide indicate that it binds biological membranes with higher affinity than the *Ec*MTS$^{256-270}$ peptide. The observed CD signal is an average over the acquisition time of the experiment, and hence it represents the time- and population-weighted average of the CD signal from the free (random coil) and bound (partly helical) peptide. If we assume that the *Ec*MTS and *Bs*MTS peptides form similar sized helices in the lipid-bound state, but the *Bs*MTS has significantly higher affinity for SUVs than the *Ec*MTS, then the CD spectrum of *Bs*MTS$^{248-268}$ will be weighted more toward the CD signature of the bound peptide and it will *appear* to be more α-helical than *Ec*MTS$^{256-270}$, as we observed experimentally. Thus, although other interpretations are possible, we take the CD spectral changes observed when the MTS peptides were incubated with SUVs as an indication that the *Bs*MTS has higher affinity for phospholipid bilayers.

Each MTS Is Tuned for Its Cognate Membrane Surface—Based on the preponderance of cationic residues on the polar face of the MTS helix (see helical wheels in Fig. 1, *A* and *C*) we hypothesized that the *E. coli* and *B. subtilis* MTSs might preferentially interact with negatively charged phospholipids such as PG and CL (27). Consistent with this hypothesis, it was recently demonstrated that full-length *Ec*MinD binds preferentially to liposomes containing anionic phospholipids (43). To test whether this property of MinD resides in the MTS, we monitored the ability of the *Ec*MTS and *Bs*MTS peptides to bind SUVs with a constant amount of PE (70%) but varying amounts of the anionic phospholipids PG and CL.

First, we examined whether anionic phospholipids are essential for MTS binding by replacing them entirely with the zwitterionic phospholipid PC. In marked contrast to the results obtained with WT-SUVs, the random coil CD spectrum of the *Ec*MTS$^{256-270}$ and *Bs*MTS$^{248-268}$ peptides was essentially unaltered by the addition of SUVs composed entirely of the zwitterionic phospholipids PE (70%) and PC (30%) (compare *black* and *green traces* in Fig. 2, *A* and *B*). In other words, these peptides do not interact with zwitterionic SUVs. We conclude that the *E. coli* and *B. subtilis* MTS can only interact with biological membranes containing anionic phospholipids.

Given the markedly different phospholipid composition of the cell membranes of *E. coli* and *B. subtilis*, we wondered whether their respective MinD MTSs, despite their small size (8–12 residues), might encode preferential interactions with *different* anionic phospholipids. Remarkably, the *Bs*MTS$^{248-268}$ peptide exhibited a distinct preference for PG over CL. This was demonstrated by the observation that PG-SUVs containing 70% PE, 30% PG induced a much stronger CD signal for this peptide than CL-SUVs comprised of 70% PE, 30% CL (compare the *blue* and *red traces* in Fig. 2*B*). The induced helicity, calculated from the ellipticity at 222 nm, was ~60% for the *Bs*MTS$^{248-268}$ peptide in the presence of PG-SUVs *versus* ~40% in the presence of CL-SUVs. We conclude that the *Bs*MTS interacts preferentially with biological membranes containing PG lipids.

In contrast to the results obtained with the *B. subtilis* MTS, the *Ec*MTS$^{256-270}$ peptide interacted equally well with PG- and CL-SUVs. The helicity induced by both types of SUVs (35–40%, see Fig. 2*A*) was not significantly different to the helicity induced by WT-SUVs (35–40%, see Fig. 1*B*) that contained a

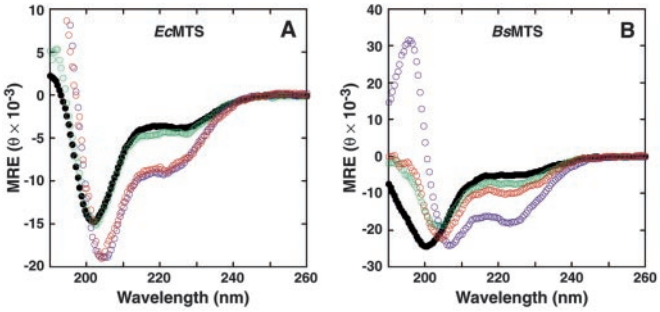

FIG. 2. **Far-UV circular dichroic spectra of *Ec*MTS$^{256–270}$ (*A*) and *Bs*MTS$^{248–268}$ (*B*) peptides in the absence of SUVs (*black*) and presence of CL-SUVs (70% PE, 30% CL, *red*), PG-SUVs (70% PE, 30% PG, *blue*), and SUVs composed entirely of zwitterionic phospholipids (70% PE, 30% PC, *green*).** The SUV:peptide molar ratio was at least 50:1 in all cases. MRE is the mean residue ellipticity in units of degrees cm^2 dmol^{-1}.

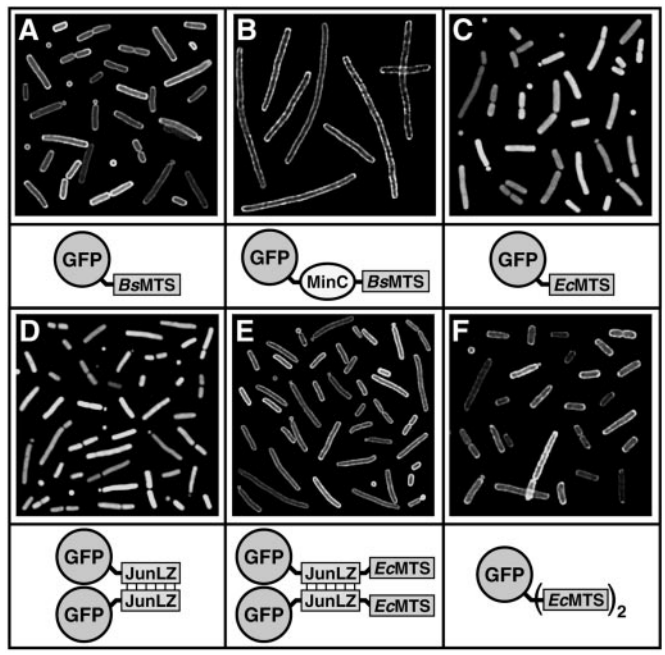

FIG. 3. **Fluorescence micrographs showing localization in *E. coli* Δ*min* strain PB114 of GFP tagged at the C terminus with various *Bs*MTS and *Ec*MTS constructs.** Cartoons of each construct are shown *below* the corresponding micrograph. JunLZ is a homodimerization-enhanced mutant of the leucine zipper motif from the c-Jun transcription factor (37). See text for details.

mixture of PG and CL. We conclude that the *Ec*MTS interacts preferentially with bilayers containing anionic phospholipids, but it has no particular preference for PG or CL.

The MinD MTS Is a Transplantable Membrane Targeting Motif—We previously showed that membrane localization of both *Ec*MinD and *Bs*MinD in an *E. coli* Δ*min* strain was dependent on the MTS (27). Deletion of as few as three C-terminal residues in the case of *Ec*MinD or five residues in the case of *Bs*MinD, as well as perturbation of the amphipathicity of the MTS helix, was sufficient to abrogate MinD localization (27). This indicates that the MTS is necessary, but not necessarily sufficient, for membrane localization of MinD. It was recently reported that GFP was not localized to the membrane when the C-terminal 40 residues of *Ec*MinD were appended to its N or C terminus (28), suggesting that other regions of *Ec*MinD may also be involved in its association with the inner membrane.

To further explore whether the MinD MTS could act as a transplantable membrane targeting motif, we examined the ability of both the *Bs*MTS and *Ec*MTS to target GFP to the membrane of the *E. coli* Δ*min* strain PB114. We showed previously that GFP alone is uniformly distributed in the cytoplasm of these cells (27). Remarkably, when the C-terminal 21 residues of *Bs*MinD were attached to the C terminus of GFP, the fusion protein was localized exclusively to the cell periphery, indicative of membrane association (Fig. 3*A*). We also examined whether the *Bs*MTS could target *Ec*MinC to the cell membrane. MinC is the proximal inhibitor of *E. coli* cytokinesis (44) but it is only active when recruited to the membrane by MinD (45). Whereas GFP-*Ec*MinC was previously shown to be cytoplasmic in *E. coli* strain PB114 (10), we found that a GFP-*Ec*MinC-*Bs*MTS fusion protein was localized exclusively to the cell periphery in this strain (Fig. 3*B*). Thus, the 21-residue *Bs*MTS is capable of targeting proteins of at least the size of the GFP-MinC fusion protein to the cell membrane. We conclude that the *Bs*MTS is an autonomous and transplantable membrane targeting motif.

Whereas strain PB114 normally displays a classical "minicelling" phenotype (*i.e.* a mixture of normal-length cells, short filaments, and minicells) because of deletion of the *minB* operon (6), we found that expression of GFP-*Ec*MinC-*Bs*MTS caused the cells to become highly filamentous, indicative of a general block to septation (Fig. 3*B*). Thus, recruitment of *Ec*MinC to the membrane using the *Bs*MTS causes the cell division inhibitory function of MinC to become activated even in the absence of MinD. It was recently proposed that, in addition to recruiting MinC to the membrane, *Ec*MinD specifically targets MinC to nascent septal complexes (46). However, the fact that MinC completely blocks septation when recruited to the membrane in a MinD-independent manner suggests that MinD-mediated targeting of MinC to septal complexes is not essential for activation of its function.

In contrast to the results obtained with *Bs*MTS, GFP remained diffusely distributed in the cytoplasm when the C-terminal 19 residues of *Ec*MinD were appended to its C terminus (Fig. 3*C*). This result supports our conclusion from the CD experiments that the *Ec*MTS has a weaker affinity for phospholipid bilayers than the *Bs*MTS. This raises the obvious conundrum of how *Ec*MinD remains stably attached to membrane prior to MinE-induced ATP hydrolysis. The experiment in which the *Ec*MTS was appended to GFP indicates that a *single* *Ec*MTS does not provide sufficient affinity for stable attachment to lipid bilayers. However, a recent report that MinD undergoes an ATP-dependent dimerization led to the suggestion that the resulting *bivalent* MTS might have significantly enhanced affinity for the membrane (28), because binding of the second MTS to the membrane would effectively be an intramolecular association.

We tested this hypothesis in two ways. First, we examined the localization of a construct in which a leucine zipper motif was inserted between the C terminus of GFP and *Ec*MTS$^{256–270}$. To ensure efficient dimerization of this GFP construct, we used an A298I mutant of the c-Jun leucine zipper that was previously shown to form more stable homodimers than the native sequence (37). A Gly-Gly-Gly linker was inserted between the leucine zipper and *Ec*MTS-encoding fragment to ensure that the orientation of the MTS was not influenced by the leucine zipper coiled coil. GFP remained cytoplasmic when tagged with just the leucine zipper motif (Fig. 3*D*), but the bivalent *Ec*MTS construct efficiently targeted GFP to the membrane (Fig. 3*E*).

In a complementary experiment, we tagged the C terminus of GFP with a tandem array of 2 or 3 copies of *Ec*MTS$^{255–270}$. Both the GFP-(*Ec*MTS)$_2$ (Fig. 3*F*) and the GFP-(*Ec*MTS)$_3$ constructs (data not shown) were mainly localized to the cell periphery. We conclude that a multivalent, but not a monovalent, *Ec*MTS can associate stably with the *E. coli* cell membrane. Interest-

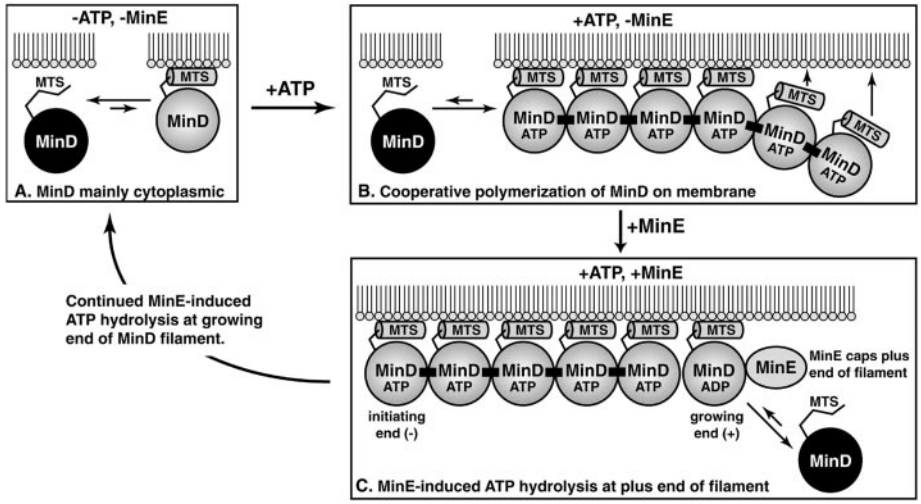

FIG. 4. **The "zipper" or cooperative polymerization model of MinD membrane association-dissociation.** *A*, nucleotide-free *Ec*MinD is monomeric and therefore has a monovalent MTS. The monovalent MTS has only moderate membrane affinity and consequently MinD is largely cytoplasmic. *B*, binding of ATP causes *Ec*MinD to polymerize cooperatively on the membrane; this could be preceded by dimerization or nucleation into short filaments prior to membrane attachment. As more MinD molecules attach to the growing, or plus, end of the MinD polymer, the MTS becomes increasingly multivalent and its affinity for the membrane increases. Thus, the MinD polymer is stably attached to the membrane bilayer. *C*, we propose that MinE first caps the plus end of the filament and prevents further growth. Second, MinE stimulates ATP hydrolysis in the MinD monomer at the plus end of the filament, thereby abolishing lateral associations (indicated by the *horizontal black bars*) between it and the residual MinD polymer. Thus, the terminal MinD molecule is converted to a monomer with a monovalent MTS, and consequently it is more likely to dissociate from the membrane than remain attached. Continued MinE-induced ATP hydrolysis at the plus end of the filament eventually results in complete depolymerization.

ingly, the peripheral localization was not as discrete for the tandem GFP-$(Ec\text{MTS})_n$ constructs as we observed with the dimeric GFP-JunLZ-EcMTS$^{256-270}$ protein. This suggests that the affinity of the *Ec*MTS-membrane interaction may depend not only on the valency of the *Ec*MTS, but also on the relative orientation of the MTSs in multivalent constructs.

DISCUSSION

The Molecular Basis of MinD Membrane Localization—It was recently shown that membrane localization of MinD requires a C-terminal MTS that is conserved across Archaea, eubacteria, and chloroplasts (27, 45). In this study, we confirmed the hypothesis (27) that the MTS interacts directly with membrane phospholipids as an amphipathic helix, with a distinct preference for anionic phospholipids. Moreover, we demonstrated that the MTSs from different bacteria interact preferentially with *different types* of anionic phospholipids, a remarkable conclusion given the small size of this motif (8–12 residues). This observation makes teleological sense, because the membrane composition of bacteria can vary significantly. Thus, we found that while the *Ec*MTS interacts preferentially with anionic phospholipids, it does not distinguish between CL and PG, consistent with the observation that there is only slightly less CL (5–10% total phospholipid) than PG (~20%) in the *E. coli* inner membrane (39, 40). In contrast, we found that the *Bs*MTS has a distinct preference for PG over CL, consistent with the fact that there are significant levels of PG (~16% of total phospholipid) and lysyl-PG (2–3%) but hardly any CL (<1%) in *B. subtilis* cell membranes (47). Thus, the polar surface of each MTS α-helix appears to have been evolutionarily tuned for interaction with specific phospholipids that are present in the inner membrane of the bacterium in which it resides. In this respect, it will be interesting in future studies to examine the lipid preferences of the MinD-MTSs from Archaea, whose membranes have a very different lipid composition to eubacteria (48). However, determination of the high-resolution structure of an MTS-phospholipid complex will probably be critical for understanding the molecular basis of MTS lipid preference.

MTS Affinity Is Tuned for Different Biological Roles—Why does a monovalent MTS from *Bs*MinD appear to be functionally autonomous while that from *Ec*MinD is not? The answer might lie in the relative membrane affinities of the two MTSs, which in turn is likely related to the quite different localization patterns and biological roles of *E. coli* and *B. subtilis* MinD. *Bs*MinD does not oscillate; it remains anchored at the cell poles by DivIVA until it is recruited to the nascent septum at a late stage in assembly of the division machinery (16, 18). Thus, *Bs*MinD appears to remain permanently attached to the cell membrane throughout the cell cycle. We suggest that the *Bs*MTS has been tuned to have very high affinity for phospholipid bilayers to facilitate the persistent association of *Bs*MinD with the cell membrane. As demonstrated in this study, the intrinsically high affinity of the *Bs*MTS for lipid bilayers enables it to behave as a transplantable membrane targeting motif that should prove to be a useful experimental tool for recruiting proteins to the cell membrane.

In contrast to the *B. subtilis* protein, *Ec*MinD undergoes a rapid pole-to-pole oscillation that persists throughout the cell cycle. This oscillation necessitates rapid cycles of membrane association-dissociation (27). ATP binding promotes association of MinD with the membrane, whereas MinE-induced ATP hydrolysis leads to release of MinD from the bilayer (23–25, 45). We postulate that an MTS with very high affinity for the bilayer would be counterproductive to such rapid attachment-detachment cycles. Rather, we suggest that the *Ec*MTS is tuned for moderate membrane affinity so that *Ec*MinD can be easily detached by MinE-induced ATP hydrolysis at the appropriate time in the oscillation cycle.

A Model for the Reversible Membrane Association of EcMinD—What is the mechanism that regulates the reversible association of the *Ec*MTS with the cytoplasmic surface of the inner membrane? We previously proposed, based on analogy with the ARF1 GTPase (49), that the hydrophobic face of the MTS helix associates with the globular core of MinD when the protein is in the ADP or nucleotide-free form, thus precluding association with the membrane. In this model, ATP binding induces a conformational change in MinD that exposes the

MTS helix and promotes association with the bilayer (27). In a variant of this model, it was proposed that the conformational change might be caused by ATP-induced dimerization of MinD, which would result in exposure of a bivalent MTS with enhanced affinity for the membrane (22, 28).

There are two problems with these models. First, they are difficult to reconcile with the observation that the C-terminal 30 residues of *A. fulgidus* MinD, which encompass the MTS, are structurally disordered when the protein is crystallized in the absence of nucleotide and lipids (38); that is, the crystal structure argues against any model in which membrane association is abrogated by a direct interaction between the MTS and the globular core of MinD. Second, although ATP-induced dimerization has been reported for *E. coli* MinD *in vitro* (28, 45), it does not occur under all conditions.[2,3] Moreover, analytical ultracentrifugation data indicate that the dimerization of *N. gonorrhoeae* MinD may be nucleotide-independent (50), which argues that ATP-induced dimerization does not regulate membrane attachment of MinD in this organism.

We propose an alternative mechanism for the reversible membrane association of *Ec*MinD that obviates both of these problems. In this model, which we refer to as the cooperative polymerization or zipper model (Fig. 4), the ADP and nucleotide-free forms of MinD are monomeric and hence possess a monovalent MTS that has only moderate affinity for the membrane. Thus, the ADP and nucleotide-free forms of MinD will be in dynamic equilibrium between the membrane and cytoplasm but the equilibrium will be heavily weighted toward the cytoplasmic population (Fig. 4*A*). As shown in this study, the MTS will be unstructured in the cytoplasmic pool of MinD and helical in the membrane-bound population. The crux of this model is that ATP-binding promotes cooperative polymerization of MinD *on the membrane*. That is, association of the ATP-bound form of MinD with the membrane induces cooperative polymerization of the protein that converts a monovalent MTS into a highly multivalent MTS. The multivalent MTS thus acts like a zipper that grows and attaches to the membrane as MinD polymerizes and thus further stabilizes the membrane-bound MinD polymer (Fig. 4*B*). Thus, ATP-induced polymerization of *Ec*MinD converts a monovalent MTS with weak membrane affinity into a polyvalent MTS with very high membrane affinity.

The MinD polymer is believed to nucleate at one of the cell poles and grow toward midcell (26, 51). MinE probably regulates MinD polymer length in at least two ways. We suggest that MinE initially "caps" the medial edge, or plus end, of the filament to block further polymer growth. This is analogous to the proposed role of SulA in rapidly blocking FtsZ polymer growth by capping preformed protofilaments (52). The absence of MinE rings and the longer than normal MinD polar zones seen in cells expressing a D45A/V49A MinE mutant (51) suggests that this mutant might be defective in the proposed filament capping function. Second, binding of MinE at the medial edge of the growing MinD polymer is thought to induce ATP hydrolysis at the tip of the MinD filament (23, 25); in the zipper model, this releases contact between the terminal MinD monomer, which is now in the ADP form, and the rest of the polymer. Thus the MinD monomer at the plus end of the filament dissociates from the membrane because the ADP form of the protein is not competent to polymerize and therefore its affinity for the membrane resides in a single MTS. In contrast, the rest of the MinD polymer remains stably attached by the polyvalent MTS zipper.

An interesting question for future studies is why MinE appears to bind primarily at the medial edge of the MinD filament. We presume that the MinD polymer, like eukaryotic actin and tubulin, is intrinsically asymmetric such that MinE can only bind to the plus end. It is well established that some proteins bind exclusively to the plus end of microtubules (53) and that several capping proteins (*e.g.* CapZ and gelsolin) bind exclusively to the barbed end of actin filaments (54). Strong evidence that the MinD polymer is polar comes from recent *in vitro* experiments indicating that MinE causes fraying at only one end of MinD protofilaments (25).

The zipper model is supported by several lines of evidence. First, a number of studies have demonstrated that *Ec*MinD assembles on lipid bilayers with positive cooperativity (23, 43) as required by the zipper model. Second, in agreement with the crystal structure of *A. fulgidus* MinD, the zipper model does not require the MTS to be shielded from the membrane or present in some alternative conformation in the ADP and nucleotide-free forms of MinD; membrane association simply depends on the valency of the MTS that in turn is determined by the level of MinD polymerization. Third, as demonstrated in this study, bivalent and trivalent *Ec*MTSs are sufficient to target GFP to the *E. coli* membrane, whereas a monovalent *Ec*MTS is not. Thus, as predicted by the zipper model, increased MTS valency leads to enhanced membrane affinity.

The reported ATP-dependent dimerization of *Ec*MinD has been taken to indicate that MinD-ATP initially associates with the membrane as a dimer (28, 45). However, the observation that ATP-MinD oligomerizes *in vitro* in the absence of lipids to form short, thin protofilaments (25) argues that short filaments rather than dimers most likely nucleate the cooperative assembly of MinD on the membrane. Although the central tenets of the zipper model do not depend on whether the basic unit of the membrane-bound MinD polymer is a monomer, dimer, or short filament, it will be important in future studies to determine whether dimerization is an essential prerequisite for cooperative polymerization of MinD on the membrane.

Acknowledgments—We thank Dr. Mary Jane Osborn for invaluable advice, Dr. Lawrence Rothfield, Dr. Debabrata RayChaudhuri, and Dr. Jo-Anne Dillon for valuable discussions, and Srdan Kobsa for contribution in the early stages of this project.

Note Added in Proof—Following acceptance of this manuscript, a complementary study was published that provides further experimental support for our proposal that the MinD membrane targeting sequence interacts with lipid bilayers as an amphipathic helix (Zhou, H., and Lutkenhaus, J. (2003) *J. Bacteriol.* **185,** 4326–4335). However, the two studies propose different molecular mechanisms for the reversible membrane association of *E. coli* MinD.

[2] A. Monroe, S. L. Rowland, and G. F. King, unpublished data.
[3] D. RayChaudhuri, personal communication.

REFERENCES

1. Erickson, H. P. (1997) *Trends Cell Biol.* **7,** 362–367
2. Harry, E. J. (2001) *Mol. Microbiol.* **40,** 795–803
3. Lutkenhaus, J. (2002) *Curr. Opin. Microbiol.* **5,** 548–552
4. Buddelmeijer, N., and Beckwith, J. (2002) *Curr. Opin. Microbiol.* **5,** 553–557
5. Errington, J., Daniel, R. A., and Scheffers, D. J. (2003) *Microbiol. Mol. Biol. Rev.* **67,** 52–65
6. de Boer, P. A. J., Crossley, R. E., and Rothfield, L. I. (1989) *Cell* **56,** 641–649
7. Rothfield, L. I., Shih, Y.-L., and King, G. F. (2001) *Cell* **106,** 13–16
8. Yu, X.-C., and Margolin, W. (1999) *Mol. Microbiol.* **32,** 315–326
9. Raskin, D. M., and de Boer, P. A. J. (1999) *Proc. Natl. Acad. Sci. U. S. A.* **96,** 4971–4976
10. Raskin, D. M., and de Boer, P. A. J. (1999) *J. Bacteriol.* **181,** 6419–6424
11. Hu, Z., and Lutkenhaus, J. (1999) *Mol. Microbiol.* **34,** 82–90
12. Rowland, S. L., Fu, X., Sayed, M. A., Zhang, Y., Cook, W. R., and Rothfield, L. I. (2000) *J. Bacteriol.* **182,** 613–619
13. Fu, X., Shih, Y.-L., Zhang, Y., and Rothfield, L. I. (2001) *Proc. Natl. Acad. Sci. U. S. A.* **98,** 981–985
14. Hale, C. A., Meinhardt, H., and de Boer, P. A. (2001) *EMBO J.* **20,** 1563–1572
15. Ramirez-Arcos, S., Szeto, J., Dillon, J.-A., and Margolin, W. (2002) *Mol. Microbiol.* **46,** 493–504
16. Marston, A. L., Thomaides, H. B., Edwards, D. H., Sharpe, M. E., and Errington, J. (1998) *Genes Dev.* **12,** 3419–3430
17. Marston, A. L., and Errington, J. (1999) *Mol. Microbiol.* **33,** 84–96
18. Harry, E. J., and Lewis, P. J. (2003) *Mol. Microbiol.* **47,** 37–48
19. de Boer, P. A. J., Crossley, R. E., Hand, A. R., and Rothfield, L. I. (1991) *EMBO*

J. **10,** 4371–4380
20. Yamaichi, Y., and Niki, H. (2000) *Proc. Natl. Acad. Sci. U. S. A.* **97,** 14656–14661
21. Gerdes, K., Møller-Jensen, J., and Jensen, R. B. (2000) *Mol. Microbiol.* **37,** 455–466
22. Lutkenhaus, J., and Sundaramoorthy, M. (2003) *Mol. Microbiol.* **48,** 295–303
23. Hu, Z., and Lutkenhaus, J. (2001) *Mol. Cell.* **7,** 1337–1343
24. Hu, Z., Gogol, E. P., and Lutkenhaus, J. (2002) *Proc. Natl. Acad. Sci. U. S. A.* **99,** 6761–6766
25. Suefuji, K., Valluzi, R., and RayChaudhuri, D. (2002) *Proc. Natl. Acad. Sci. U. S. A.* **99,** 16776–16781
26. Shih, Y.-L., Le, T., and Rothfield, L. (2003) *Proc. Natl. Acad. Sci. U. S. A.* **100,** 7865–7870
27. Szeto, T. H., Rowland, S. L., Rothfield, L. I., and King, G. F. (2002) *Proc. Natl. Acad. Sci. U. S. A.* **99,** 15693–15698
28. Hu, Z., and Lutkenhaus, J. (2003) *Mol. Microbiol.* **47,** 345–355
29. Shoemaker, K. R., Kim, P. S., York, E. J., Stewart, J. M., and Baldwin, R. L. (1987) *Nature* **326,** 563–567
30. Bernstein, L. S., Grillo, A. A., Loranger, S. S., and Linder, M. E. (2000) *J. Biol. Chem.* **275,** 18520–18526
31. Chen, Y.-H., Yang, J. T., and Chau, K. H. (1974) *Biochemistry* **13,** 3350–3359
32. Chang, C. T., Wu, C.-S. C., and Yang, J. T. (1978) *Anal. Biochem.* **91,** 13–31
33. Johnson, J. E., and Cornell, R. B. (1994) *Biochemistry* **33,** 4327–4335
34. Dunne, S. J., Cornell, R. B., Johnson, J. E., Glover, N. R., and Tracey, A. S. (1996) *Biochemistry* **35,** 11975–11984
35. Huang, H., Ball, J. M., Billheiner, J. T., and Schroeder, F. (1999) *Biochemistry* **38,** 13231–13243
36. Cormack, B. P., Valdivia, R. H., and Falkow, S. (1996) *Gene* (*Amst.*) **173,** 33–38
37. Bains, N. P. S., Wilce, J. A., Mackay, L. G., and King, G. F. (1999) *Lett. Pept. Sci.* **6,** 381–390
38. Cordell, S. C., and Lowe, J. (2001) *FEBS Lett.* **492,** 160–165
39. Dowhan, W. (1998) *Biochim. Biophys. Acta* **1376,** 455–466
40. de Kruijff, B., Killian, J. A., Rietveld, A. G., and Kusters, R. (1997) *Curr. Top. Membr.* **44,** 477–515
41. Wieprecht, T., Apostolov, O., Beyermann, M., and Seelig, J. (1999) *J. Mol. Biol.* **294,** 785–794
42. Wang, G., Peterkofsky, A., and Clore, G. M. (2000) *J. Biol. Chem.* **275,** 39811–39814
43. Mileykovskaya, E., Fishov, I., Fu, X., Corbin, B., Margolin, W., and Dowhan, W. (2003) *J. Biol. Chem.* **278,** 22193–22198
44. de Boer, P. A. J., Crossley, R. E., and Rothfield, L. I. (1992) *J. Bacteriol.* **174,** 63–70
45. Hu, Z., Saez, C., and Lutkenhaus, J. (2003) *J. Bacteriol.* **185,** 196–203
46. Johnson, J. E., Lackner, L. L., and de Boer, P. A. (2002) *J. Bacteriol.* **184,** 2951–2962
47. Matsumoto, K., Okada, M., Horikoshi, Y., Matsuzaki, H., Kishi, T., Itaya, M., and Shibuya, I. (1998) *J. Bacteriol.* **180,** 100–106
48. Shimada, H., Nemoto, N., Shida, Y., Oshima, T., and Yamagishi, A. (2002) *J. Bacteriol.* **184,** 556–563
49. Goldberg, J. (1998) *Cell* **95,** 237–248
50. Szeto, J., Ramirez-Arcos, S., Raymond, C., Hicks, L. D., Kay, C. M., and Dillon, J. A. (2001) *J. Bacteriol.* **183,** 6253–6264
51. Shih, Y. L., Fu, X., King, G. F., Le, T., and Rothfield, L. I. (2002) *EMBO J.* **21,** 3347–3357
52. Cordell, S. C., Robinson, E. J., and Lowe, J. (2003) *Proc. Natl. Acad. Sci. U. S. A.* **100,** 7889–7894
53. Howard, J., and Hyman, A. A. (2003) *Nature* **422,** 753–758
54. Cooper, J. A., and Schafer, D. A. (2000) *Curr. Opin. Cell Biol.* **12,** 97–103

The MinD Membrane Targeting Sequence Is a Transplantable Lipid-binding Helix

Tim H. Szeto, Susan L. Rowland, Cheryl L. Habrukowich and Glenn F. King

J. Biol. Chem. 2003, 278:40050-40056.
doi: 10.1074/jbc.M306876200 originally published online July 25, 2003
